Cell. Mol. Biol. (ISSN: 1165-158X)

Journal Homepage: www.cellmolbiol.org

Cellular and Molecular Biology

Original Article

The fibroblast heterogeneity across keloid, normal and tumor samples from single-cell resolution

Xia Wang[1,#], Weihu Huang[2,#,*], Yongtie Li[3], Chen Zhu[4]

[1] *Department of Pathology, Ji'an Central People's Hospital, Ji'an, Jiangxi, China*
[2] *Department of Medical Cosmetology, Ji'an Central People's Hospital, Ji'an, Jiangxi, China*
[3] *Department of Burn Injury, Ji'an Central People's Hospital, Ji'an, Jiangxi, China*
[4] *Ji'an Central People's Hospital, Ji'an, Jiangxi, China*

Article Info

Article history:

Received: April 06, 2024
Accepted: March 51, 2024
Published: July 31, 2024

Use your device to scan and read the article online

Abstract

Keloids are defined as a benign dermal fibroproliferative disorder, with excessive fibroblast proliferation, and excessive overproduction of collagen. Although the heterogeneity during keloid development has been extensively studied, the heterogeneity across different skin states is still unclear. So, a global comparison across skin states is needed. In this study, we collected samples from 5 states of skin, including melanoma, cutaneous squamous cell carcinoma, keloid skin, scar skin, and healthy control samples. The heterogeneity of cell types and subtypes was analyzed and compared across 5 states, and we observed significant differences among them. Our results showed a cancer-like fibroblast, which is not in normal samples, may play an important role in antigen processing and presentation. We also noticed that the mesenchymal fibroblast increased in keloid samples, which highly expressed POSTN. And POSTN may participate in epithelial-mesenchymal transition and collagen overexpression to promote keloid growth. These findings help to understand the alteration among different skin states and provide potential genetic basis for keloid therapies.

Keywords: Keloid, Fibroblast, Single cell RNA-sequencing.

1. Introduction

Keloid is a skin disease that can be characterized by fibroblast hyperproliferation and excessive accumulation of extracellular matrix. During the healing process of wound, the keloid loses normal constraints and control over collagen synthesis metabolism. Previously, keloids are usually classified as harmless skin growths, the keloids demonstrate biological features similar to malignant tumors [1], such as excessive proliferation, resistance to apoptosis, and invasive behavior. Interestingly, recent statistical research demonstrated the overall cancer risk was 1.49-fold higher in the keloid group compared to healthy control group. When regarding skin-related cancers, the risk of keloid group is higher (Relative risk = 1.73) [2].

Previous studies have proved the alterations of fibroblasts in keloid samples, and they determined the dysregulated pathways, regulators and ligand-receptor interactions in keloid fibroblasts, as well as several potential targets for medical therapies [3]. Other studies comparing keloid and scar groups also showed the fibroblast can be divided into 4 subpopulations: secretory-papillary, secretory-reticular, mesenchymal and pro-inflammatory [4,5].

Although there are several studies that discovered the inner changes in keloid, melanoma and other skin diseases, comparative insight among different skin states is still needed. To uncover the heterogeneity among different states of skin, we collected normal, scar, keloid and tumor samples (melanoma and cutaneous squamous cell carcinoma). Comparative analyses were performed to demonstrate the heterogeneity of cell types and subtypes in different skin states.

2. Materilas and Methods

2.1. Sample collection

A total of three single cell RNA-seq datasets were used, containing five groups, which were downloaded from the gene expression ombinous (GEO), with accession numbers of GSE163973 (Keloid and normal scar samples), GSE144240 (cutaneous squamous cell carcinoma and normal samples), GSE72056 (melanoma samples).

2.2. Single-cell RNA sequencing (scRNA-seq) data processing

All cells were extracted from the full datasets, filtered

* Corresponding author.
E-mail address: huangwh9912@163.com (W. Huang).
# These authors contributed equally
Doi: http://dx.doi.org/10.14715/cmb/2024.70.7.29

the tumor cells based on the cell type annotation provided by the authors, and then handled by Seurat [6]. Before analysis, the normal cells were filtered to remove low-quality cells with high and low (>6000 and <200) UMI-counts. Also, the mitochondrial genes were removed.

The cells from different datasets were integrated directly. The gene expression for each cell was normalized by log-transformation and refined by a scale factor of 10000. Then the liner dimension reduction, here we used principal component analysis, was performed using different dimensions, to determine the elbow point (k=9). Harmony was used to eliminate the batch effects caused by different samples [7]. Cells were used to construct a structural SNN graph, and then clustered by modifying the Louvain community detection method. Finally, the clustering results were visualized using the uniform manifold approximation and projection for dimension reduction (*UMAP*).

2.3. Calculation of correlation coefficient score

Based on the various cell type fractions in different projects, we evaluated the Pearson correlation coefficient score between different projects. A score close to 1 means a positive correlation and the score close to -1 means a negative correlation.

2.4. Calculation of cell-cycle score

To quantify the cell-cycle state in different fibroblast subpopulations, we adopted the S- and G2/M-phased gene sets from previous study [8], and calculated the cell cycle scores by Seurat. Each cell will be assigned a score, as well as the predicted classification in either G2M, S or G1 phase, based on its expression of G2/M and S phase markers.

2.5. Detection of differential expressed genes

For specific clusters, the differential expressed genes were detected by "FindMarkers", with other clusters as background. To obtain more global and exact changes for each cluster, we only kept the genes with Foldchange>1 and required the percentage of candidate genes more than 0.25. Further, the Wilcox test was performed to filter the genes with adjusted *P*-value (Bonferroni correction) below 0.05.

2.6. Gene ontology and KEGG enrichment analysis

Before enrichment analysis, the gene symbols were transformed to ENTREZID, by clusterProfiler v4.8 [9]. Gene ontology functional enrichment, as well as KEGG enrichment of DEGs at $P<0.05$ was analyzed using clusterProfiler. The candidate enrichment results were filtered by a cutoff of *P*-value below 0.05, and adjusted *P*-value below 0.05, refined by "BH" method.

2.7. Gene set enrichment analysis

Gene Set Enrichment Analysis (GSEA) was also conducted using clusterProfiler v4.8. The gene sets and molecular signatures were obtained from the Molecular Signatures Database [10]. A threshold of adjusted *P*-value<0.05 is used to filter final gene set. Finally, the whole results were visualized by GseaVis.

2.8. Statistical analysis

This study utilized Pearson correlation coefficients for analyzing relationships between cell fractions, and the Wilcoxon test for identifying differentially expressed genes, adjusting significance with Bonferroni correction ($P < 0.05$). Cell-cycle states were analyzed via gene set scoring. Gene Ontology (GO) and Kyoto Encyclopedia of Genes and Genomes (KEGG) enrichment analyses, alongside Gene Set Enrichment Analysis (GSEA), identified significant pathways and gene sets (adjusted $P < 0.05$), employing the clusterProfiler package for comprehensive statistical evaluations.

3. Results

3.1. Single-cell RNA-seq reveals cell heterogeneity of different skin states

The improvement of high throughput technology, such as single-cell RNA sequencing, provides a novel, detailed way to understand the cellular heterogeneity in various states of skin. We collected the scRNA datasets from melanoma (MEL), cutaneous squamous cell carcinoma (CSCC), keloid skin (KS), scar skin (SS), and healthy control (HC) samples. After stringent filtration, a total of 89,805 normal cells are obtained. To reduce the batch effects, the single-cell data were integrated with Harmony and then clustered by Uniform Manifold Approximation and Projection (*UMAP*) (Figure 1A). To address the cell types of 19 clusters more precisely, we calculated the marker genes of each cluster, and combined those in previous study, and then annotated the 19 clusters as 6 cell types (Figure 1A, B, C) [11-13]. The epithelial cells were based on the expression of *KRT14* and *KRT5*, endothelial cells were *PECAM1* and *CDH5*, smooth muscle cells were *ACTA2* and *RGS5*, fibroblast cells were *PDGFRA* and *PDGFRB*, immune cells were *PTPRC*, and melanocytes were *MLANA* (Figure 1C).

We next observed the dynamic cell proportions in different skin states (Figure 1D). When compared to HC and tumor (MEL and CSCC) samples, KS and SS samples have more fibroblast cells, endothelial cells, and smooth muscle cells. These alterations have also been reported to be one reason for the abnormal development of keloid and

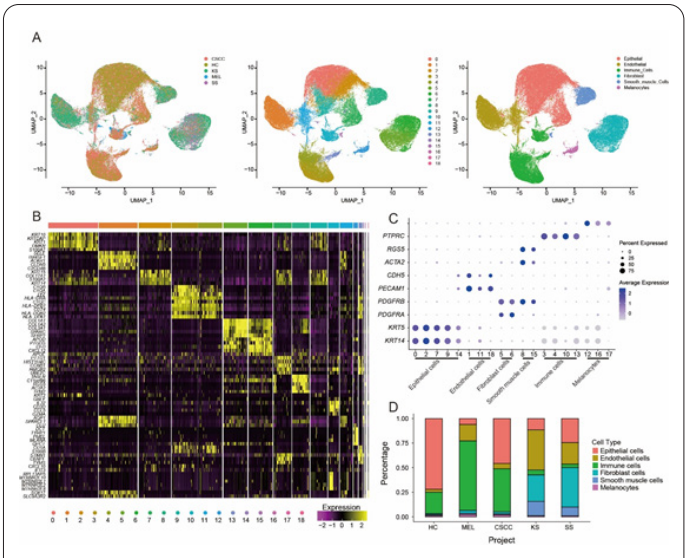

Fig. 1. Overview of integrated cells from 5 skin states. (A) U M A P for all integrated cells, clustered by project id (left), cluster id (middle), and annotated cell types(right). (B) The differential expressed genes among 19 clusters. (C) Dot plot showing the expression of known marker genes in each cell cluster. (D) Cell fractions of cell types in 5 skin states.

scar [4,14,15]. Also, the changes in immune cell proportion, especially for lymphocytes, may reflect the different skin states. The tumor samples have more immune cells, indicating immune infiltration, while the keloid and scar samples have less proportion.

3.2. The subtypes of fibroblast cells various in different skin states

To further understand the functional changes of fibroblast cells in skin diseases, we extracted fibroblast cells from the integrated dataset, and re-cluster these cells into 8 subtypes (Figure 2A, B). Notably, the HC samples only have 1 subtype c4, we named this subtype as normal fibroblast, which can be marked by *MMP1* and *MMP3*, *WNT5A* (Figure 2B). Tumor samples (MEL and CSCC) have 2 fibroblast subtypes, c4 and c7 (Figure 2B). The cluster c7 didn't exist in the normal samples (Figure 2B), so we named c7 as cancer-like fibroblast, which is highly expressed *TK1* and *MKI67* and *SPC25* (Figure 2D). And the fraction of c7 is also distinct in different cancer types (MEL: 82.2%; CSCC: 1.6%). Besides tumor samples, this cancer-like fibroblast also exists in KS (1.1%) and SS (0.68%) samples, close to the fraction in CSCC. In the correlation statistics, KS and SS were more similar, than healthy and tumor samples (Figure 2C), which may suggest the different skin states.

A total of 252 specific expressed genes of c7 were found (percentage of expressed cells more than 0.25, and $\log_2$ fold change 0.5), when comparing c7 and other clusters. 242 pathways were significantly enriched in GO enrichment analysis (Figure 2D). The results showed that the antigen processing and presenting, as well as MHC II protein-related cascades, may be the key functional changes for the cancer-like fibroblast.

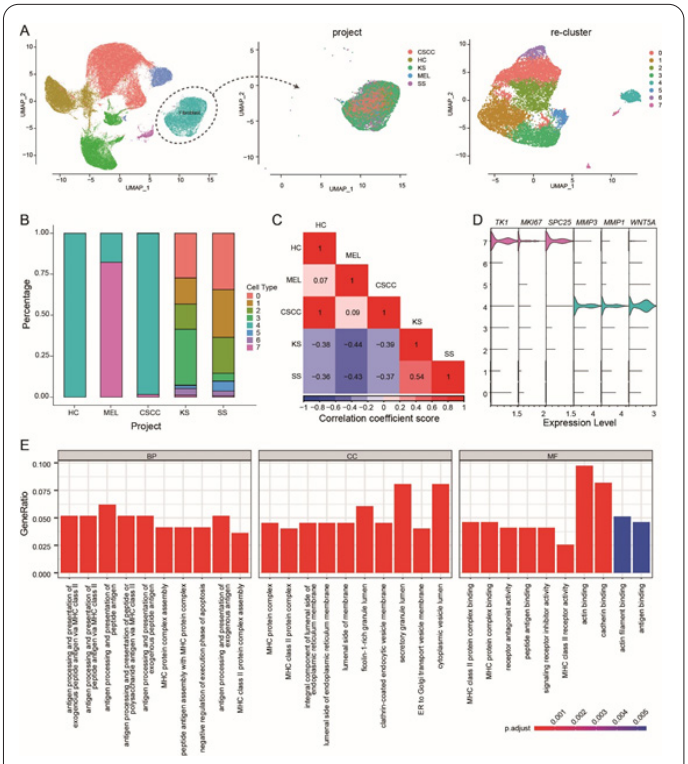

Fig. 2. Differences between subtypes of fibroblasts. (A) UMAP for fibroblast cells (middle) extracted from all cells (left), and the re-cluster results for the 14,292 cells. (B) Cell fractions of fibroblast subtypes in 5 skin states. (C) The correlation coefficient scores between the fibroblasts of the 5 skin states. (D) Marker genes of normal fibroblast subtype (c4) and cancer-like fibroblast subtype (c7). (E) GO enrichment results of the specific expressed genes of cancer-like fibroblast subtype.

3.3. The specific fibroblast subtypes in keloid and scar

To demonstrate the differences between KS and SS samples, we removed the normal fibroblast c4 and cancer-like fibroblast c7. Referring to previous study, the fibroblasts in keloid can be divided into secretory-papillary, secretory-reticular, mesenchymal, and pro-inflammatory subtypes [5]. Secretory-papillary fibroblasts are generally located in the papillary, comprising *APCDD1*, *AXIN2*, *COLEC12*, *PTGDS*, and *COL18A1*, the reticular fibroblast located in the reticular dermis, with markers genes such as *MFAP5* and *WISP2* [5]. Mesenchymal fibroblasts can be defined by some mesenchymal progenitor markers, such as *COL11A1* and *POSTN*, which may correspond to skeletal system development, ossification, or osteoblast differentiation. The signatures of pro-inflammatory fibroblasts contain *APOE*, *CCL19* and *CXCL13* [4,5].

Based on these known markers, the 13,336 cells can be divided into 4 subtypes, c0 and c6 are pro-inflammatory fibroblast, c1 is secretory-reticular fibroblast, c2 is secretory-papillary fibroblast, c3 and c5 is mesenchymal fibroblast (Figure 3A, C). The clustering and cell fraction results are similar to previous study, supporting the robustness of results [4].

Among these 4 subtypes of fibroblast, the mesenchymal fibroblast increased in keloid compared to normal scar, showing the greatest changes in cell fraction, from 10.8% in SS to 36.6% in KS. And mesenchymal fibroblast is the only subtype whose cell fraction increased in KS, while other 3 subtypes all decreased (Figure 3B). Further

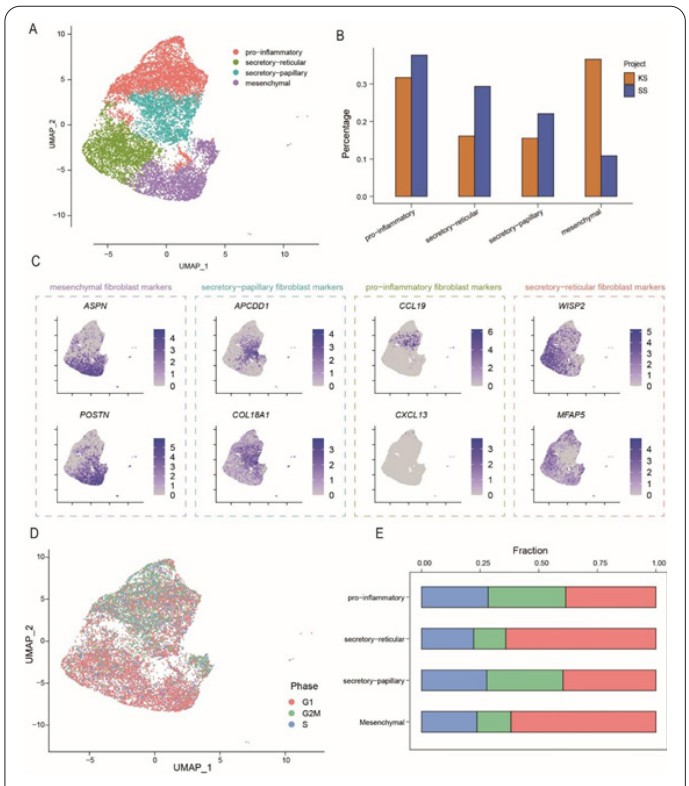

Fig. 3. Annotation of fibroblast subtypes in keloid and scar samples. (A) UMAP for annotated fibroblast subtypes. (B) Bar plot showed the proportion differences for the four fibroblast subtypes between KS and SS. (C) Feature plots showed the marker genes expression of 4 fibroblast subtypes. (D) The cell cycle phases of fibroblasts are shown in a UMAP plot. (E) Cell fractions of cell cycle phases in 4 fibroblast subtypes.

analysis of cell cycle score showed mesenchymal and secretory-reticular fibroblast has less cells in G2M phase, compared with pro-inflammatory and secretory-papillary fibroblasts, suggesting these subtypes may be proliferating (Figure 3D, E).

3.4. The potential roles of mesenchymal fibroblast in abnormal skin

To explore the characteristics and function of mesenchymal fibroblasts, we compared them with other clusters and defined 170 cluster-specific highly expressed genes. When focused on the genes with great expression differences, we found *POSTN*, *FN1*, *MDK*, with a $\log_2$ fold change of 3.69, 2.34, and 1.89. *POSTN* encodes a secreted extracellular matrix protein that functions in tissue development and regeneration, including wound healing, and ventricular remodeling following myocardial infarction [16,17]. And *POSTN* was reported to promote the expression of collagens in keloid samples [4].

Based on GO and KEGG enrichment, a total of 155 and 16 catalogues were significant, respectively (Figure 4A, B). Notably, the extracellular matrix organization and collagen organization-related pathways showing high enrichment degrees, such as "collagen-containing extracellular matrix" (GO: 0062023), showing the highest rich factor (0.32) with a low adjusted *P*-value ($5.95*10^{-44}$). Functional enrichment results also demonstrate the changes correlated with mesenchymal fibroblast. The catalog "Focal adhesion" (hsa04510, adjusted *P*-value = $1.14*10^{-9}$, rich factor = 0.23) was also reported to play an important role in clustering integrin receptors interact with the extracellular matrix on the outside of cells and with the actin cytoskeleton [18]. Similarly, "ECM-receptor interaction" is also engaged in the mesenchymal fibroblast-specific expressed genes (hsa04512, adjusted *P*-value = $6.24*10^{-12}$, rich factor = 0.20).

When considering the gene order of fold changes, the GSEA results only showed two categories, "Epithelial-Mesenchymal Transition" and "Myogenesis" (Figure 4C). "Epithelial Mesenchymal Transition" catalog owned an NES value of 2.46, a low FDR value of $1.81*10^{-7}$. It includes 26 genes, while the highest is *POSTN1*, and second is *FN1*. "Myogenesis" contains 5 genes (*COL1A1*, *COL3A1*, *SPARC*, *ADAM12*, *TAGLN*), less than "Epithelial-Mesenchymal Transition", with an NES score of 1.61, and an FDR value of 0.016. These results may suggest the significant influence in alterations of the transition of epithelial-mesenchymal and myogenesis, but a greater importance of the former, rather than the latter.

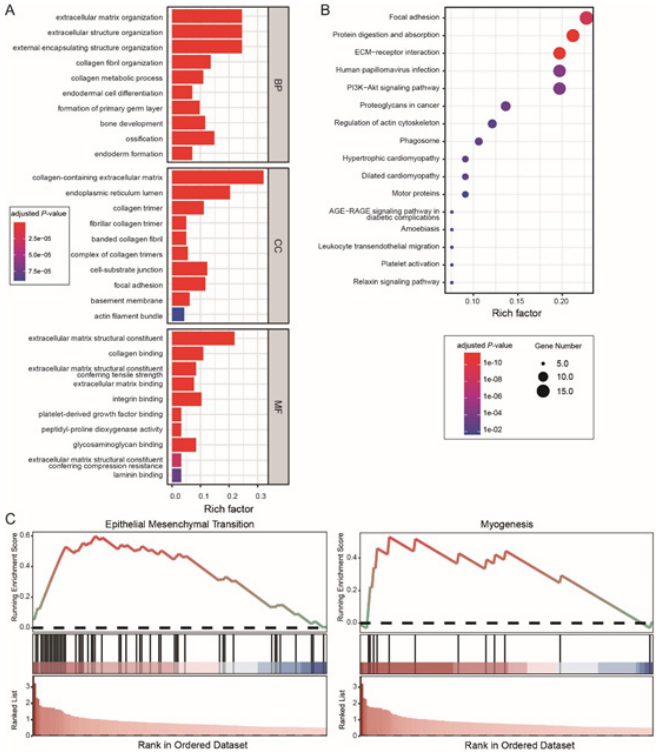

Fig. 4. Functional changes of mesenchymal fibroblast. (A) Gene ontology enrichment results of mesenchymal fibroblast-specific expressed genes, separated by 3 domains, biological progress, cell component and molecular function. (B) KEGG functional enrichment results of mesenchymal fibroblast specific expressed genes. (C) Gene set enrichment analysis for mesenchymal fibroblast-specific expressed genes.

4. Discussion

In skin tissues, keloid is regarded as a beginning disease, but consistent with non-malignant dermal tumors phenotypically, due to the excessive fibroblast proliferation, and excessive overproduction of collagen which never metastasizes [19]. As one key component of skin, fibroblasts have been evidenced to participate in many skin diseases. For instance, cancer-related fibroblast may additionally participate in the inflammatory response of the tumor site by releasing a variety of chemokines and cytokines in melanoma [20] and might support the growth and metastasis of tumors by inhibiting lymphocyte infiltrate on and remodeling the tumor extracellular matrix in CSCC and so on [21]. Although we have realized the importance of fibroblast in development and treatment of skin disease, there is little research that clarifies the cell heterogeneities in different skin states, globally. In this study, we collected a total of 89,805 cells in 5 different skin states (HC, MEL, CSCC, KS, SS), and explained the dynamic alteration of cell clusters and sub-clusters, as well as the key genes and pathways during the alteration. These findings will provide a more global insight into skin diseases, as well as a genetic basis for therapy application.

Firstly, we demonstrated the cell heterogeneities among five skin states and found the proportion of immune cells, especially for lymphocytes, in keloid and scar samples, are far below normal and tumor samples. In previous research, inflammation may be one cause for keloid. Several studies have suggested an increase in pro-inflammatory mediator expression in keloids [22], and several inflammatory cell types are prominent in keloids, particularly mast cells and macrophages [23,24]. There is one research that found an increased fraction of lymphocytes in keloid samples, but the increasing fraction is fluctuating [25]. This finding is slightly different from previous study, which may explain the abnormal development of keloid, without supervision by lymphocytes. But this may be a result of cells dropping out due to the limitation of single cell RNA-sequencing technology, or the individual heterogeneities.

And then, we found the great differences of fibroblast subtypes in various skin states. Such as one cancer-like fibroblast, which does not exist in normal skin. Then functional enrichment results showed that this subtype may participate in antigen processing and presentation. This cancer-like fibroblast has been found in CSCC, KS, and SS samples, and KS has a higher fraction closer to CSCC,

which may indicate the malignance of KS. But the correlation statistics showed a distinct state between KS and SS, compared with normal and tumor samples. These findings may reflect the abnormal state of keloid, malignant but distinguished from tumor samples. Further, a larger dataset may help us to uncover more details, and explain the mechanism.

Finally, when comparing the fibroblast subpopulations between keloid and scar, we found a higher cell-cycle score of mesenchymal fibroblasts, as well as the greatest fraction changes, which are evidenced by previous studies [4]. When focusing on the mesenchymal fibroblasts, one gene, *POSTN*, attracted our attention, this gene has been proven to promote the expression of collagens in fibroblasts. Another research also found *POSTN* highly expressed in cancer-related fibroblast, enriched around CSCC, which may also indicate the cancer-like character of keloid [21]. Furthermore, the functional enrichment showed significant alterations in the transition of epithelial-mesenchymal and myogenesis.

In conclusion, we compared the multiple states of skin, from single-cell resolution, and demonstrated the heterogeneity of cell types and subtypes. The global integration and comparison help us to understand the dynamic changes of skin more clearly, and contribute to designing clinical therapy from genetic basis.

5. Conclusions

Our study demonstrated the keloid sample is malignant but absolutely different compared with tumor samples. Also, found the key altered fibroblasts in keloid, and mesenchymal fibroblasts, as well as their main changes in transition of epithelial mesenchymal and myogenesis. These findings provided a clear insight into understanding skin development, especially for wound healing.

Conflict of interests

The author has no conflicts with any step of the article preparation.

Consent for publications

The author read and approved the final manuscript for publication.

Ethics approval and consent to participate

No human or animals were used in the present research.

Informed consent

The authors declare that no patients were used in this study.

Data availability

The data used in this study are publicly available and allow unrestricted reuse through open licenses. All datasets in this study were downloaded from the gene expression ombinous (GEO) database, with an access link: https://www.ncbi.nlm.nih.gov/geo/.

Authors' contributions

Huang Weihu designed the study and was responsible for the reliability of the submitted results. Wang Xia did the data analysis and drafted the manuscript. Li Yongtie and Zhu Chen help to revise the manuscript. All authors have read and agreed to the published version of the manuscript.

Funding

This study was supported by 2024 Jiangxi Provincial Health and Health Committee Science and Technology Plan Project (202410999).

References

1. Mari W, Alsabri SG, Tabal N, Younes S, Sherif A, Simman R (2015) Novel Insights on Understanding of Keloid Scar: Article Review. J Am Coll Clin Wound Spec 7:1-7. doi: 10.1016/j.jccw.2016.10.001
2. Lu YY, Tu HP, Wu CH, Hong CH, Yang KC, Yang HJ et al (2021) Risk of cancer development in patients with keloids. Sci Rep-Uk 11:9390. doi: 10.1038/s41598-021-88789-1
3. Liu X, Chen W, Zeng Q, Ma B, Li Z, Meng T et al (2022) Single-Cell RNA-Sequencing Reveals Lineage-Specific Regulatory Changes of Fibroblasts and Vascular Endothelial Cells in Keloids. J Invest Dermatol 142:124-135. doi: 10.1016/j.jid.2021.06.010
4. Deng CC, Hu YF, Zhu DH, Cheng Q, Gu JJ, Feng QL et al (2021) Single-cell RNA-seq reveals fibroblast heterogeneity and increased mesenchymal fibroblasts in human fibrotic skin diseases. Nat Commun 12:3709. doi: 10.1038/s41467-021-24110-y
5. Sole-Boldo L, Raddatz G, Schutz S, Mallm JP, Rippe K, Lonsdorf AS et al (2020) Single-cell transcriptomes of the human skin reveal age-related loss of fibroblast priming. Commun Biol 3:188. doi: 10.1038/s42003-020-0922-4
6. Butler A, Hoffman P, Smibert P, Papalexi E, Satija R (2018) Integrating single-cell transcriptomic data across different conditions, technologies, and species. Nat Biotechnol 36:411-420. doi: 10.1038/nbt.4096
7. Korsunsky I, Millard N, Fan J, Slowikowski K, Zhang F, Wei K et al (2019) Fast, sensitive and accurate integration of single-cell data with Harmony. Nat Methods 16:1289-1296. doi: 10.1038/s41592-019-0619-0
8. Tirosh I, Izar B, Prakadan SM, Wadsworth MN, Treacy D, Trombetta JJ et al (2016) Dissecting the multicellular ecosystem of metastatic melanoma by single-cell RNA-seq. Science 352:189-196. doi: 10.1126/science.aad0501
9. Wu T, Hu E, Xu S, Chen M, Guo P, Dai Z et al (2021) clusterProfiler 4.0: A universal enrichment tool for interpreting omics data. Innovation (Camb) 2:100141. doi: 10.1016/j.xinn.2021.100141
10. Subramanian A, Tamayo P, Mootha VK, Mukherjee S, Ebert BL, Gillette MA et al (2005) Gene set enrichment analysis: a knowledge-based approach for interpreting genome-wide expression profiles. P Natl Acad Sci Usa 102:15545-15550. doi: 10.1073/pnas.0506580102
11. Kalucka J, de Rooij L, Goveia J, Rohlenova K, Dumas SJ, Meta E et al (2020) Single-Cell Transcriptome Atlas of Murine Endothelial Cells. Cell 180:764-779. doi: 10.1016/j.cell.2020.01.015
12. Belote RL, Le D, Maynard A, Lang UE, Sinclair A, Lohman BK et al (2021) Human melanocyte development and melanoma dedifferentiation at single-cell resolution. Nat Cell Biol 23:1035-1047. doi: 10.1038/s41556-021-00740-8
13. Pu W, Shi X, Yu P, Zhang M, Liu Z, Tan L et al (2021) Single-cell transcriptomic analysis of the tumor ecosystems underlying initiation and progression of papillary thyroid carcinoma. Nat Commun 12:6058. doi: 10.1038/s41467-021-26343-3
14. Macarak EJ, Wermuth PJ, Rosenbloom J, Uitto J (2021) Keloid disorder: Fibroblast differentiation and gene expression profile in fibrotic skin diseases. Exp Dermatol 30:132-145. doi: 10.1111/exd.14243
15. Andrews JP, Marttala J, Macarak E, Rosenbloom J, Uitto J (2016) Keloids: The paradigm of skin fibrosis - Pathomechanisms and treatment. Matrix Biol 51:37-46. doi: 10.1016/j.mat-

bio.2016.01.013
16. Bonnet N, Garnero P, Ferrari S (2016) Periostin action in bone. Mol Cell Endocrinol 432:75-82. doi: 10.1016/j.mce.2015.12.014
17. Li A, Wei Y, Hung C, Vunjak-Novakovic G (2018) Chondrogenic properties of collagen type XI, a component of cartilage extracellular matrix. Biomaterials 173:47-57. doi: 10.1016/j.biomaterials.2018.05.004
18. Burridge K (2017) Focal adhesions: a personal perspective on a half century of progress. Febs J 284:3355-3361. doi: 10.1111/febs.14195
19. Tan S, Khumalo N, Bayat A (2019) Understanding Keloid Pathobiology From a Quasi-Neoplastic Perspective: Less of a Scar and More of a Chronic Inflammatory Disease With Cancer-Like Tendencies. Front Immunol 10:1810. doi: 10.3389/fimmu.2019.01810
20. Papaccio F, Kovacs D, Bellei B, Caputo S, Migliano E, Cota C et al (2021) Profiling Cancer-Associated Fibroblasts in Melanoma. Int J Mol Sci 22:7255. doi: 10.3390/ijms22147255
21. Ou Z, Lin S, Qiu J, Ding W, Ren P, Chen D et al (2022) Single-Nucleus RNA Sequencing and Spatial Transcriptomics Reveal the Immunological Microenvironment of Cervical Squamous Cell Carcinoma. Adv Sci 9:e2203040. doi: 10.1002/advs.202203040
22. Zhang Q, Yamaza T, Kelly AP, Shi S, Wang S, Brown J et al (2009) Tumor-like stem cells derived from human keloid are governed by the inflammatory niche driven by IL-17/IL-6 axis. Plos One 4:e7798. doi: 10.1371/journal.pone.0007798
23. Dong X, Zhang C, Ma S, Wen H (2014) Mast cell chymase in keloid induces profibrotic response via transforming growth factor-beta1/Smad activation in keloid fibroblasts. Int J Clin Exp Patho 7:3596-3607.
24. Wilgus TA (2020) Inflammation as an orchestrator of cutaneous scar formation: a review of the literature. Plast Aesthet Res 7:54. doi: 10.20517/2347-9264.2020.150
25. Boyce DE, Ciampolini J, Ruge F, Murison MS, Harding KG (2001) Inflammatory-cell subpopulations in keloid scars. Br J Plast Surg 54:511-516. doi: 10.1054/bjps.2001.3638